

## Adsorption of Kr, Xe, and Ar on highly uniform MgO smoke

Jean-Paul Coulomb,\* Timothy S. Sullivan, and Oscar E. Vilches  
*Department of Physics, University of Washington, Seattle, Washington 98195*

(Received 9 July 1984)

The first atomic layer of Kr, Xe, and Ar adsorbed on MgO smoke is explored by using adsorption isotherms. A procedure has been developed by which we produce MgO smoke powders of higher homogeneity than previously reported. On these powders, apparent two-dimensional (2D) solid-vapor, fluid-vapor, and solid-fluid coexistence regions are observed for Kr and Xe. Triple-point temperatures are estimated to be  $66.6 \pm 0.5$  K and  $100.8 \pm 1.0$  K, and the critical temperatures are estimated to be  $86.8 \pm 1.0$  K and  $119 \pm 2.0$  K, respectively, for these two elements. A comparison between Kr and Xe 2D-solid densities at the fluid-solid transition suggests that the 2D-solid phases are incommensurate with the substrate. The Ar isotherms are qualitatively different from those of Kr and Xe, showing no features corresponding to 2D phase transitions in the  $P$ - $T$  range studied. A qualitative estimate places the Ar 2D critical temperature at about 65 K.

### I. INTRODUCTION

Most highly homogeneous surfaces currently used for thermodynamic studies of physical adsorption have either triangular or honeycomb lattices of adsorption sites. Typical examples are basal-plane graphite (exfoliated graphite, Grafoil, Union Carbide ZYX, graphite foam, etc.), boron nitride, lamellar halides (double halides), and graphite plated with rare gases. Possible phases of adsorbed films, the character of phase transitions among them, the existence of critical and triple points and their temperatures, and the growth of bulk properties are, for a given adsorbate, strongly dependent on the crystallographic structure, the lattice parameters, and the adsorption potential of the substrate.<sup>1-3</sup>

It is well known that the equilibrium surface of an MgO crystal is a (100) plane.<sup>4</sup> Crystals intentionally cut in other orientations will reconstruct to that plane after moderate heat treatment although forming a stepped surface. <sup>4</sup>He atomic beam diffraction studies show that (100) MgO has an adsorption potential dominated by the (00) and (10) Fourier coefficients, thus providing a square array of potential minima with the periodicity of the MgO lattice.<sup>5,6</sup> A preliminary calculation<sup>7</sup> shows that for all the rare gases the minimum in the adsorption potential is on top of a Mg ion. If localized adsorption of rare gases were to occur on this lattice, for all of them except Xe (too large) only half of the sites would be occupied due to the relative sizes of the adsorber and adsorbate. At melting this would provide a good realization of the two-dimensional (2D) Ising order-disorder transition as contrasted with the three-state Potts transition actively studied on graphite surfaces.<sup>8-11</sup> If, on the other hand, the adsorption was not localized, MgO would provide a square symmetry substrate for adsorption of an incommensurate (triangular symmetry) monolayer. The melting transition of a solid 2D layer on this substrate may be Isinglike.<sup>12</sup>

The reasons for using MgO smoke for thermodynamic studies are its relatively large specific area and that upon electron microscope examination the smoke particles appear to consist primarily of single-crystal cubes with only the (100) surface exposed.<sup>13</sup> These crystals vary in size from about 200 to 2000 Å. A few years ago Dash *et al.* reported using adsorption isotherms of Kr on MgO at liquid-nitrogen temperature to find the right procedure for obtaining powders with a uniform surface.<sup>14</sup> Various experiments have since used powders prepared following that procedure.<sup>15-17</sup> Recently we have been able to produce MgO smoke of much higher homogeneity than previously reported.<sup>18</sup> Utilizing this MgO we have studied the first-layer adsorption characteristics of Kr, Ar, and Xe in a temperature range consistent with vapor pressures in the (0.001–10)-Torr range. This range, for Kr and Xe, appears to be sufficient for determining 2D liquid-vapor and solid-fluid coexistence regions and critical and triple temperatures.

Other authors have studied adsorption of rare gases on powder substrates with cubic symmetry. In particular Ross and Clark,<sup>19</sup> Fisher and McMillan,<sup>20</sup> and Takaishi and Mori<sup>21</sup> have performed extensive measurements using various gases and ionic crystals such as NaCl, NaBr, KCl, and RbCl. All of these crystals have a considerably larger lattice parameter than MgO. A more important aspect for adsorption studies, however, is that none of these substrates appear to have been produced with the surface homogeneity possible to attain with MgO. While this work was in progress we became aware of an x-ray diffraction study of Kr on MgO.<sup>22</sup> The results of the diffraction work will allow us to calculate the total area of our sample and to deduce the structure of a monolayer Xe solid film as well as to conjecture that the Ar films are liquidlike at monolayer completion in our temperature range, while they are probably solid at much lower temperatures.<sup>17</sup> This article briefly describes the surface preparation procedure and the apparatus used for obtaining the adsorption isotherms, followed by details and discussion of our measurements.

## II. EXPERIMENTAL PROCEDURE

A description of the detailed study that led to the preparation of the MgO substrate has been published.<sup>18</sup> A brief summary of the techniques used is given here.

One to four Mg ribbons (Matheson, Coleman, and Bell) 0.010×0.110×12 in. long were burned in static air. Only the smoke that rose and coated a clean aluminum surface was collected. We noted that the transferring of this sample to a quartz bulb for heat treatment (at about 950°C) under vacuum ( $P$  less than  $1 \times 10^{-6}$  Torr) should be done in a relatively short time (less than 5 min). When this was done, the vertical step observed in the first layer of many Kr/MgO isotherms at liquid-nitrogen temperature grew considerably in size, and a second smaller step appeared within that same first layer, as shown in Figs. 1(a)–1(c). To sort out the reason for this improvement we also prepared MgO by burning the ribbon in dry O<sub>2</sub>/Ar mixtures of varying composition in a glove box. Although the samples collected in this way were very small, the 77-K isotherms were the best ones measured (see Fig. 1) as judged by the size and verticality of the first step and the curvature of the very low coverage portion before the step. With this experience we concluded that it is likely that the quality of most large (several grams) smoke samples used in previous experiments, all prepared in air, have at best a surface that will yield isotherms like the one shown in Fig. 1(a) or Ref. 14, and not as good as the samples used for this study. This degradation must be associated with formation of Mg(OH)<sub>2</sub> by moist-air exposure to such an extent that baking and thermal decomposition cannot reconstruct uniform large (100) surfaces for adsorption. This conclusion is consistent with the rather poor isotherms obtained by direct thermal decomposition of Mg(OH)<sub>2</sub>.

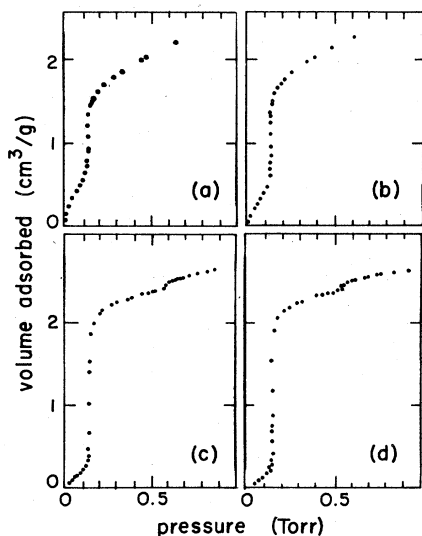


FIG. 1. Kr/MgO isotherms at liquid N<sub>2</sub> temperatures for four different samples. (a), (b), and (c): Samples prepared in static air placed in vacuum system 80, 22, and 5 min, respectively, after preparation. (d) Sample prepared in 20%O<sub>2</sub>/80 vol. % Ar mixture. All samples baked at least 24 h at 950°C after being placed in vacuum system.

For the measurement of the adsorption isotherms of Sec. III, samples of about 0.15 g of smoke made in air were attached to a high-vacuum system within 5 min of production. After baking for over 24 h at  $\sim 950^\circ\text{C}$  and  $P < 10^{-6}$  Torr, the oven was removed and a CTi Model 21 cryogenic refrigerator<sup>23</sup> was attached to the quartz bulb containing the sample with a graphite-vacuum grease paste for thermal contact. Care was taken to completely enclose the quartz bulb with a copper container and a heat shield (as well as a vacuum enclosure). In spite of these precautions we believe that a small temperature gradient may still be present in the sample since isotherms obtained by immersion of the quartz bulb in liquid nitrogen show steps that are slightly more vertical than the same steps obtained at the same temperature with the refrigerator. Nevertheless, the refrigerator is extremely useful since one can change temperatures with ease. The temperature stability of our unit is approximately 0.01 K over the time necessary to complete an isotherm ( $\sim 10$  h).

The isotherms were measured by dosing from a calibrated volume using a 10-Torr full-scale MKS baratron<sup>24</sup> capacitance gauge. Although the minimum scale readings of this unit is  $10^{-3}$  Torr, relative measurements can be made which are ten times better by use of an external digital voltmeter. For most of the isotherms the temperature was determined at the end of each run by condensing the appropriate gas on the bulb until the equilibrium pressure did not change any more. The temperature was then obtained from published vapor-pressure tables.<sup>25</sup> We also calibrated a diode attached to the refrigerator against the vapor pressure and used this calibration for some of the isotherms.

The gases used were (a) Kr, Airco grade 4.5 (99.995% purity), (b) Xe, Linde research grade 4.5 (99.995% purity), and (c) Ar, Linde research grade 5.5 (99.9995% purity). A thermomolecular pressure correction was made (only significant for  $P < 2$  Torr) using Takaishi and Sensui's formula.<sup>26</sup>

## III. RESULTS

Adsorption isotherms for Kr are shown in Fig. 2. The lowest temperature at which we measured an isotherm was dictated by the pressure measurement sensitivity. The unbaked portions of the glass vacuum system and Baratron heads have an outgassing rate of about 0.001 Torr/h. Equilibration times for each point vary between points but are  $\sim 15$  min; the powder sample we use is totally uncompressed so gas diffusion through it is easy. Equilibration times are much longer on compressed powders. For practical reasons we limited most of our measurements to the first monolayer and the beginning of the second-layer step. A complete isotherm at liquid-nitrogen temperature shows at least three large vertical steps indicating a minimum of three-layers formation at that temperature.

We show, on a semilogarithmic scale in Fig. 3, a  $P$  versus  $1/T$  possible phase diagram for this system deduced from the location of the quasivertical steps on the isotherms of Fig. 2. The straight lines through the points have been drawn as guides to the eye. The data points

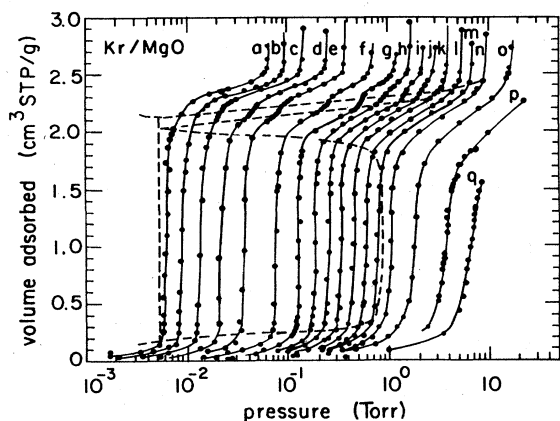


FIG. 2. Kr/MgO isotherms. The amount adsorbed is specified as the volume of ideal gas at STP adsorbed per gram of MgO sample. Isotherm temperatures: (a) 66.76, (b) 67.82, (c) 69.10, (d) 70.97, (e) 72.56, (f) 75.21, (g) 77.47, (h) 78.97, (i) 80.28, (j) 81.59, (k) 83.16, (l) 84.52, (m) 85.87, (n) 87.56, (o) 90.88, (p) 95.21, and (q) 98.66 K. Dashed lines indicate estimated phase boundaries determined as described in text.

represent, for each isotherm, the following features: (a) the pressure at the density in the middle of the "first"-layer large vertical riser [determined by estimating the center of the riser for each isotherm below the critical temperature (defined below) and averaging over all isotherms], (b) the pressure at the inflexion point on the small substep (sub) between the first and second layer, (c) the pressure of the low portion of the second-layer riser, and (d) the "bulk" three-dimensional (3D) saturation vapor pressure of Kr, the property measured to determine the temperature of the isotherm. The line called first on Fig. 3 ends at a point we believe to be the 2D liquid-vapor critical point,  $T_c(2D) = 86.8 \pm 1.0$  K. This temperature was estimated by constructing from the isotherms a graph of  $(\partial \log_{10} P / \partial n)_{n_c}$  versus  $T$  where the derivative is taken for all the isotherms at the critical density as determined

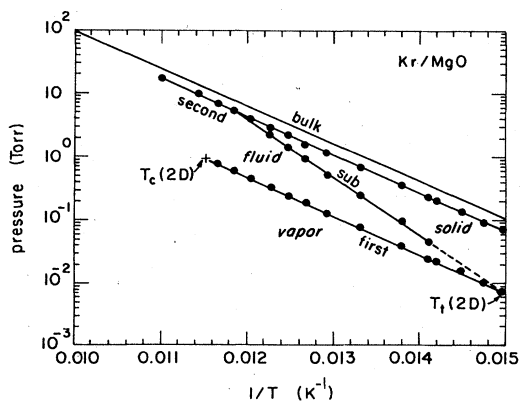


FIG. 3.  $P$  vs  $1/T$  diagram for Kr/MgO and vapor pressure of 3D Kr. The monolayer critical and triple points and various adsorbed phases are indicated. First, sub, and second correspond to pressure and temperature pairs taken respectively from the first-layer large step, the melting-line smaller step, and the second-layer step in the isotherms of Fig. 2.

in (a) above. This method has been used extensively by Larher<sup>27</sup> to determine 2D critical temperatures for a large number of systems. For a perfect system, below  $T_c(2D)$  the slope should be zero, while above  $T_c(2D)$  the slope increases, the departure from zero thus being taken as the critical temperature. For a real system inhomogeneities (finite size and energy variations in the adsorbing potential) lead to finite inverse logarithmic slopes below  $T_c(2D)$  and profound rounding effects near and at  $T_c(2D)$ , so the method is not very accurate. This is the reason for the relatively large error associated with our determination.

The line called sub on Fig. 3 runs into the first line at  $66.6 \pm 0.5$  K, a temperature slightly below our lowest isotherm and quite a bit below the isotherm for which we were able to resolve the substep. Following our interpretation of the results, we believe this to be the triple-point temperature,  $T_t(2D)$  for this system.

On the high-temperature end, the sub line will run into the second-layer vertical riser. We did not pursue the study of this merging or two-layer regime.

Adsorption isotherms for the Xe/MgO systems are shown in Fig. 4, with the  $P$  versus  $1/T$  semilogarithmic plot (obtained in the same manner as for Kr) shown in Fig. 5. A comparison between the Kr and Xe diagrams shows qualitatively the same features, with  $T_c(2D) = 119 \pm 2$  K and  $T_t(2D) = 100.8 \pm 1$  K, both temperatures obtained by a procedure similar to that described above for Kr. These temperatures are very similar to those observed in the Xe/graphite system.<sup>28-31</sup>

Adsorption isotherms for the Ar/MgO system are shown in Fig. 6. It is obvious that no substep is present on any of the isotherms, so the  $P$ -versus- $1/T$  diagram shown in Fig. 7 has no sub line and consequently no triple point. In addition, the first-layer vertical riser has a larger inverse logarithmic slope than for the Kr or Xe isotherms below  $T_c(2D)$ , and shows only a slight increase of this slope as the temperature is increased to isotherm pressures at the upper limit of our measuring range. Thus we

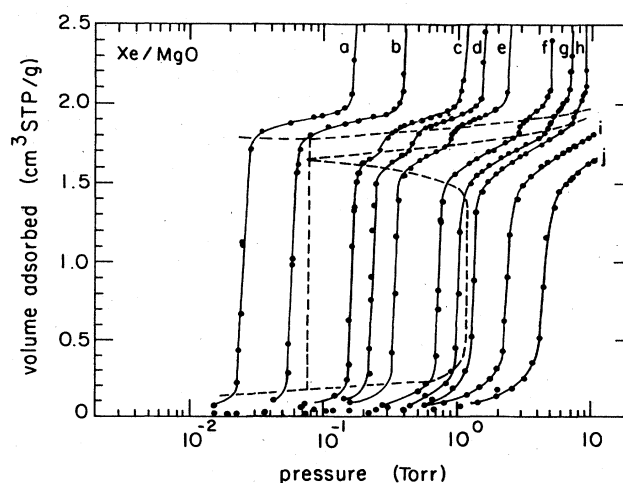


FIG. 4. Xe/MgO isotherms. Temperatures: (a) 96.86, (b) 100.47, (c) 106.20, (d) 108.44, (e) 111.02, (f) 116.14, (g) 118.72, (h) 121.15, (i) 126.17, and (j) 131.19 K. Dashed lines indicate estimated phase boundaries determined as described in text.

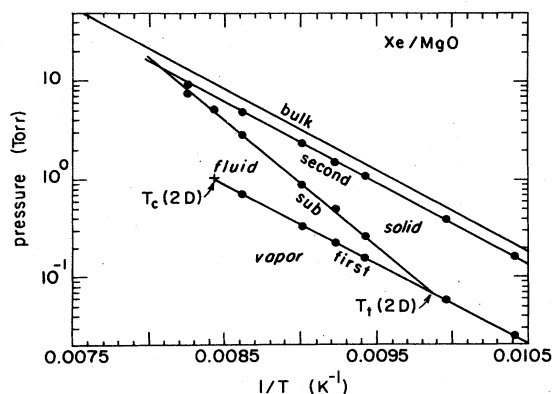


FIG. 5.  $P$  versus  $1/T$  diagram showing features for Xe/MgO, and vapor pressure of 3D Xe. Various monolayer phases and the critical and triple points are shown.

also find no strong evidence for a 2D critical point in the range studied. Nevertheless our discussion below points towards the existence of a liquid phase in the range studied, with a critical temperature in the vicinity of 65 K.

#### IV. DISCUSSION

In Table I we compare our results to a sample of those obtained by other authors for the same adsorbates on different substrates. In particular it is interesting to place our results on the broader picture developed by Larher and collaborators<sup>27,32</sup> for the adsorption on double halides where the (triangular) lattice parameter of the adsorber can be varied over a wide range, and also compare them to results on graphite where a large amount of both thermodynamic and structural data exists. In the double-halide adsorbents the dimensional incompatibility  $I = (a - d)/d$ , where  $a$  is the crystalline parameter of the sublattice of sites and  $d$  is the distance between nearest neighbors in the (111) plane of the 3D adsorbate, plays a very important role producing large variations in the critical and tri-

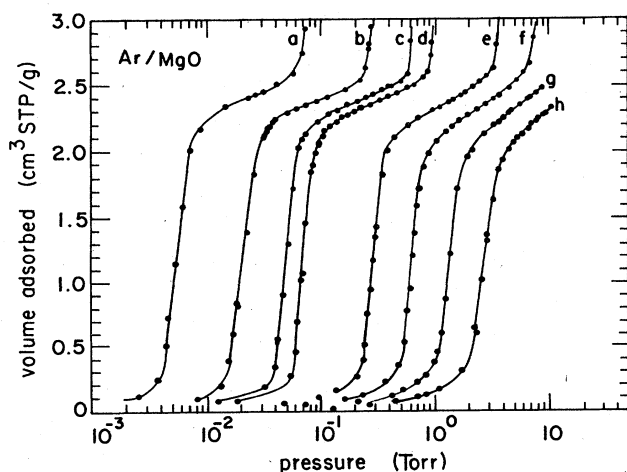


FIG. 6. Ar/MgO isotherms. Temperatures: (a) 48.22, (b) 51.47, (c) 53.95, (d) 55.35, (e) 59.43, (f) 62.54, (g) 65.59, and (h) 68.78 K.

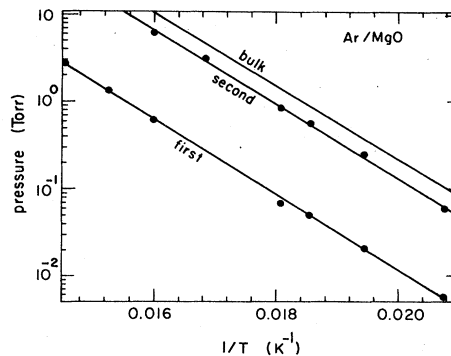


FIG. 7.  $P$  versus  $1/T$  diagram showing first- and second-layer steps for Ar/MgO, and vapor pressure of 3D Ar.

ple temperatures. When  $I = 0$ , the adsorbate and adsorber would be perfectly compatible. The closer the system gets to this condition the higher (with some small deviations) are the  $T_t$  and  $T_c$  observed. It seems important to interpret our results to try to decide whether our films are commensurate or not.

The recent x-ray scattering measurements of Jordan *et al.*<sup>22</sup> on Kr/MgO show below  $\sim 67$  K a slightly compressible 2D incommensurate triangular solid with nearest-neighbor distance very close to that of the (111) planes of solid 3D Kr for similar temperatures. Their measurements cover the range between 20 and 120 K and from about 0.45 to 1.11 incommensurate layers. The  $\sim 67$ -K constant melting temperature they observe is the same as that determined in this study for the triple temperature within experimental error. We believe that due to the higher surface homogeneity of the present sample to that used in the x-ray experiment, we are also able to track the solid-fluid coexistence line up to the point where it merges into the second layer. The results of Jordan *et al.* give a surface density of  $0.0657 \text{ \AA}^{-2}$  at 67 K. Thus we can use this solid density at the triple line to obtain the adsorption area of our MgO samples and a density scale for all our measurements.

It is possible to compare the densities at melting of a Kr and a Xe isotherm. The two isotherms chosen, shown in Fig. 8, are at comparable relative temperatures using

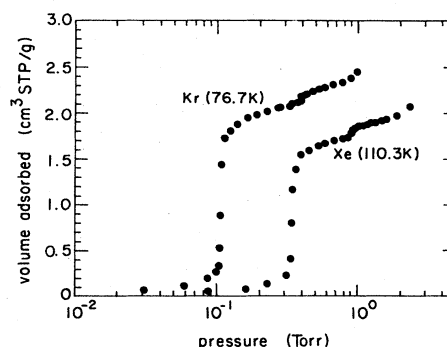


FIG. 8. Kr and Xe isotherms used for solid monolayer density comparison.

TABLE I. Temperatures (in K) of 2D triple and critical points for Xe, Kr, and Ar adsorbed on various substrates. MgO data from this work.  $I = (a - d)/d$  is the dimensional incompatibility (in %); comm. is the commensurate structure that preempts the critical and triple points; n.a. (not applicable) means that the substrate has square symmetry. Question mark indicates uncertainty.

Substrate	Xe			Kr			Ar		
	$T_t$	$T_c$	$I$	$T_t$	$T_c$	$I$	$T_t$	$T_c$	$I$
Graphite	99 <sup>a</sup> 100 <sup>e</sup>	117 <sup>a</sup>	-3.5	comm. <sup>b</sup>	comm. <sup>b</sup>	+ 4.6	50 <sup>c</sup> 47.9 <sup>b</sup> 47.2 <sup>d</sup>	55 <sup>d</sup>	+ 12.3
BN	102 <sup>f</sup>	119 <sup>f</sup>			87 <sup>f</sup>				
NiCl	99 <sup>g</sup>	112 <sup>h</sup>	-21.0		81 <sup>h</sup>	-14.4		58 <sup>h</sup>	-8.8
CoCl	99 <sup>g</sup>	114 <sup>h</sup>	-19.6						
FeCl	99 <sup>g</sup>	112 <sup>h</sup>	-18.5					63 <sup>h</sup>	-5.8
CdCl		113 <sup>h</sup>	-12.8		90 <sup>h</sup>	-5.7		79 <sup>h</sup>	-0.3
CdBr								83 <sup>h</sup>	+ 3.3
PbI								60.5 <sup>h</sup>	+ 19.4
MgO	100.8	119	n.a.	66.6 67.0 <sup>i</sup>	86.8	n.a.	< 48	65(?)	n.a.
KCl					76.0 <sup>j</sup>	n.a.			
RbCl					75.5 <sup>j</sup>	n.a.			

<sup>a</sup>A. Thomy and X. Duval, *J. Chim. Phys.* **67**, 1101 (1970).

<sup>b</sup>J. P. McTague, J. Als-Nielsen, J. Bohr, and M. Nielsen, *Phys. Rev. B* **25**, 7765 (1982). Not interpreted by these authors as a triple point.

<sup>c</sup>F. Millot, *J. Phys. (Paris) Lett.* **40**, L9 (1979).

<sup>d</sup>A. D. Migone, Z. R. Li, and M. H. W. Chan, *Phys. Rev. Lett.* **53**, 810 (1984).

<sup>e</sup>J. A. Litzinger and G. A. Stewart, in *Ordering in Two Dimensions*, edited by S. K. Sinha (Elsevier, New York, 1980), p. 267.

<sup>f</sup>J. Regnier, A. Thomy, and X. Duval, *J. Colloid Interface Sci.* **70**, 105 (1979).

<sup>g</sup>C. Tessier and Y. Larher, in *Ordering in Two Dimensions*, Ref. e, p. 163.

<sup>h</sup>F. Millot, Y. Larher, and C. Tessier, *J. Chem. Phys.* **76**, 3327 (1982).

<sup>i</sup>J. L. Jordan, J. P. McTague, L. Passell, and J. B. Hastings, *Bull. Am. Phys. Soc.* **28**, 874 (1983).

<sup>j</sup>T. Takaishi and M. Mohri, *J. Chem. Soc., Faraday Trans. I*, **68**, 1921 (1972).

$T_c(2D)$  for scaling. Taking surface coverages slightly above solidification for both elements (2.23 cm<sup>3</sup>/g for Kr and 1.86 cm<sup>3</sup>/g for Xe for this smoke sample) we get a ratio of 1.20 for the 2D solids at melting. Using the densities<sup>33</sup> for 3D Kr at 75 K and Xe at 110 K we get from the nearest-neighbor distances (4.06 Å for Kr and 4.43 Å for Xe) a ratio of surface densities for close-packed structures of 0.0701 Å<sup>-2</sup>/0.0589 Å<sup>-2</sup>=1.19. This ratio is essentially the same as the experimental ratio for the coverages. Thus we conclude that Xe also forms a triangular incommensurate lattice on MgO.

The Ar results are more difficult to interpret, but they may point towards a large liquid-vapor coexistence region. Table I shows for Ar a very large variation of  $T_c$  with the various substrates, while at the same time  $T_t$  is normally below the pressure range easily accessible for studies of adsorption isotherms on powder samples with high-vacuum equipment. The best high-resolution study of Ar/graphite using heat-capacity techniques have recently yielded a triple-point temperature of 47.2 K,<sup>34</sup> in reasonable agreement with scattering and isotherm measurements (although the scattering measurements disagree in the interpretation).<sup>31</sup> Our lowest temperature isotherm was taken at 48.2 K, and at this temperature the accuracy in the pressure measurements is relatively poor. Thus all our measurements may have been taken above the solidification temperature.

The critical temperature could have been in the tem-

perature range measured. The logarithmic slope of the isotherms, although in all of them much larger than for Kr and Xe, increases slightly for the highest two temperatures we measured. By using this increase and comparing with the actual variation of the inverse slopes for the other two gases near  $T_c$ , we can conjecture that the critical temperature is in the vicinity of 65 K. This value is relatively high for a fluid with large incompatibility, and thus may be also high (see Table I), for a completely incommensurate system, but it is not totally unreasonable.

Additional support for the existence of the liquid phase comes from considering the ratios of either a close-packed plane of solid (at 55 K) or liquid (at  $T_t$ ) 3D Ar to that of solid-Kr highest-density planes such as the above. They are 1.14 and 1.01, respectively. The ratio of the Ar monolayer density (2.25 cm<sup>3</sup>/g for  $T=55$  K) to the solid-Kr monolayer density (2.23 cm<sup>3</sup>/g for  $T=75$  K) is 1.01, the same as the liquid-Ar-to-solid-Kr ratio. Using the close-packed solid ratios, the substep indicating crossing of the solid-fluid melting line should have been around 2.54 cm<sup>3</sup>/g for our sample. This coverage is very close to the start of the second-layer step in the temperature range surveyed, and thus a substep would have been very difficult to observe.

The final possibility that Ar/MgO form a commensurate structure, thus not showing critical or triple points (like Kr/graphite) seems unlikely since the commensurate density (0.0564 Å<sup>-2</sup>) would occur at about 1.79 cm<sup>3</sup>/g in

our sample. This surface density is well within the first vertical riser.

If our interpretation is correct, the solid-liquid coexistence region could exist over a very small temperature range on the first monolayer and would not extend to much higher temperature than  $T_i$ , a phenomena with analogs in films of other substances on graphite. [For example, in  $O_2$  (Refs. 35–37) the solid “ $\delta$ ” phase-liquid-vapor  $T_i \cong 26$  K and the liquid-vapor  $T_c \cong 65$  K, but the  $\delta$ -phase monolayer melting line goes up to only 32 K, well below the volumetric isotherms range ( $T \lesssim 55$  K).]

A characteristic of the isotherms that we are unable to account for is the large difference in the slopes of the first vertical step between Ar on one side and Kr and Xe on the other side. Dash and Puff,<sup>38</sup> and Ecke, Dash, and Puff<sup>39</sup> have developed a theoretical model for incorporating the effect of inhomogeneities due to variations in substrate binding and/or finite sizes into the free energy of the film. From this free energy one can calculate the chemical potential of the adsorbate and since at equilibrium  $\mu_f = \mu_v$  and  $\mu_v = kT \ln(P\lambda^3/kT)$  for the very low density (ideal gas) 3D vapor that corresponds to the measured pressure, variations in the chemical potential of the film will be reflected in variations in the equilibrium pressure. Thus heterogeneities produce finite slopes in the isotherms measured over a film two-phase coexistence region. For a perfect substrate  $\Delta P/P = 0$ , while for an imperfect substrate,  $\Delta P/P = \Delta\mu_f/kT = -\Delta\epsilon/kT$ , where  $\Delta\epsilon$  is the variation in substrate binding for the particular film being considered. Dash and Puff developed a simple way of relating the slopes of the isotherms at coexistence for various substances on the same substrate, namely,

$$\left( \frac{\partial \ln P}{\partial N} \right)_{T,A}^{(1)} = \frac{\epsilon_0^{(1)}}{\epsilon_0^{(2)}} \left| \frac{n_2^{(2)} - n_1^{(2)}}{n_2^{(1)} - n_1^{(1)}} \right| \frac{T^{(2)}}{T^{(1)}} \left( \frac{\partial \ln P}{\partial N} \right)_{T,A}^{(2)}, \quad (1)$$

where  $\epsilon_0^{(1)}$  is the single-particle binding energy,  $n_2^{(1)}$  and  $n_1^{(1)}$  are the densities of the two phases in coexistence, and  $T^{(1)}$  is the temperature at which the isotherm is being taken, all the quantities for species (1), with similar meanings for species (2). From the isosteric heats described below we have estimated the single-particle (zero coverage) binding energies to be approximately 840, 1100, and 1400 K for Ar, Kr, and Xe, respectively. Using the average slope for all the isotherms in the two-phase region, and taking the temperatures and densities for the two phases at approximately the middle of the two-phase liquid-vapor coexistence region (54, 77, and 111 K), we estimate that the Xe slope should be 1.19 times the Kr slope, and the Ar slope 0.99 times the Kr slope. The actual experimental ratios are 0.94 and 2.64, respectively. The Xe/Kr ratio is within the scatter of the average slope determination (about 25%). The Ar/Kr ratio is completely outside the uncertainties. One possibility for this discrepancy is that the Ar film is strongly affected by this substrate (orientation or partial commensuration), while Kr and Xe are not. This would render the comparison using (1) not appropriate since epitaxy effects were not considered in the Dash and Puff model. Equation (1) is a simplification of a more general equation that includes the isothermal compressibilities of the adsorbed film. An estimate of the

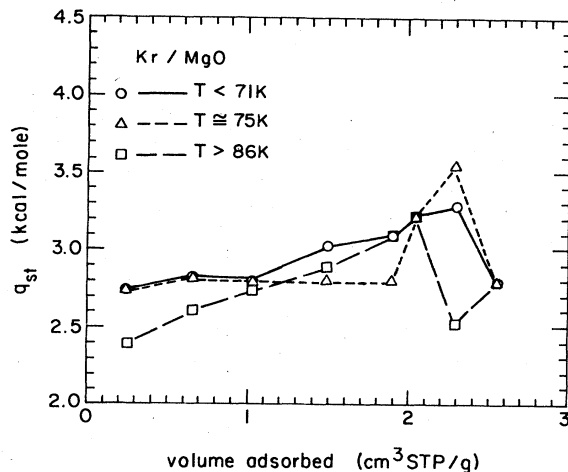


FIG. 9. Representative average latent heats of adsorption at constant coverage versus coverage for three temperature regimes for Kr/MgO, determined from  $P$  vs  $1/T$  constant coverage plots. Lines are guides to the eye. The line (—□—) was determined in a single-surface phase region for  $V < 2$  cm<sup>3</sup> STP/gram.

neglected term using the 3D compressibilities does not account for the experimental difference in slopes.

The latent heat of adsorption of the monolayers at constant coverage

$$q = kT^2 \left( \frac{\partial \ln P}{\partial T} \right)_N \quad (2)$$

can be calculated from the data by taking pressure and temperature differences between contiguous isotherms along an isostere. If the isostere is taken in a single-surface phase region, the latent heat defined by (2) is the isosteric heat of adsorption  $q_{st}$ .<sup>40</sup> We have observed that this method, while giving considerable detail, also produces considerable scatter from isotherm to isotherm due to small absolute errors in  $T$  that translate into large errors in  $\Delta T$ . At very low coverages, in addition, small absolute errors in coverage produce very large changes in the equilibrium pressure, so the zero-coverage isosteric heat

TABLE II. Estimates of the zero-density binding energies and average latent heats of adsorption ( $\pm 5\%$ ) at various isotherm features.

	Ar	Kr	Xe
$\epsilon_0/k$ (K)	840	1100	1400
First-layer, large step (liquid-vapor)			
$q$ (kcal/mole)	1.98	2.79	3.72
First-layer, sub step (fluid-solid)			
$q$ (kcal/mole)		4.18	5.88
Second-layer step			
$q$ (kcal/mole)	1.95	2.77	3.76

(from which the single-particle binding energy can be calculated) is difficult to determine. Thus it is sometimes more accurate to make semilogarithmic graphs of  $P$  versus  $(1/T)$  for different constant coverages, whose slopes give  $q/k$  (or  $q_{st}/k$ ). Figure 9 shows three latent heat of adsorption curves at different constant temperatures versus coverage for Kr determined in this second way. The extrapolation of the 87.56-K curve (single-surface phase) to  $V=0$  gave  $q_{st}^0=2.25$  kcal/mole from which we estimated the zero-coverage binding energy

$$\epsilon_0 = q_{st}^0 - \frac{1}{2}kT \quad (3)$$

reported in Table II. Similar determinations for Ar and Xe (see Table II) were used in Eq. (1) to estimate the slopes. Equation (3) assumes at zero coverage a 2D classical gas with a vibrational degree of freedom perpendicular to the substrate.<sup>41</sup> Results are also shown in Table II for heats of adsorption representative of other features of the isotherms. The values of  $\epsilon_0/k$  and  $q_{st}$  for Ar, Kr, and Xe/MgO are substantially lower than values reported for the same adsorbates on BN or graphite.<sup>42</sup> For example, in the case of Xe which appears to have a similar phase dia-

gram on the three substrates, the  $\epsilon_0/k$  for BN is approximately 1810 K, while for graphite it is about 1980 K. On MgO we find it to be about 1400 K. The first-step heats of adsorption (within the liquid-vapor region) are 4.20 and 5.01 kcal/mole, respectively, while for MgO it is about 3.72 kcal/mole. Thus MgO appears to be a much weaker substrate for adsorption than either BN or graphite.

#### ACKNOWLEDGMENTS

The authors thank Professors J. G. Dash and M. Bienfait for many helpful discussions and suggestions, and for strong encouragement while doing this work. We are grateful to Dr. Jean Jordan for sharing her x-ray results with us a long time before they were ready for publication. We also thank Professor S. C. Fain, Jr., and Professor M. W. Cole for a careful reading and criticism of an earlier version of the manuscript. This work was supported by the National Science Foundation under Grant No. DMR-81-16421, the Centre National de la Recherche Scientifique—National Science Foundation (CNRS-NSF) (J.-P.C.) and an NSF-CNRS cooperative Grant (No. INT-82-12501).

\*Permanent address: Département de Physique, Faculté des Sciences de Luminy, Université d'Aix-Marseille II, Case Postale 901, F-13288 Marseille (Cédex) 9, France.

<sup>1</sup>For a very recent review of various aspects of physical adsorption, see papers presented at the Symposium on the Statistical Mechanics of Adsorption, Trieste, Italy, 1982 [Surf. Sci. 125, 1 (1983)].

<sup>2</sup>M. Bienfait, P. Thorel, and J. P. Coulomb, *Surface Mobilities on Solid Materials*, edited by V. T. Binh (Plenum, New York, 1983), p. 257.

<sup>3</sup>O. E. Vilches, Ann. Rev. Phys. Chem. 31, 463 (1980).

<sup>4</sup>V. E. Henrich, Surf. Sci. 57, 355 (1976).

<sup>5</sup>K. H. Rieder, Surf. Sci. 118, 57 (1982).

<sup>6</sup>G. Brusdeylins, R. B. Doak, J. G. Skofronick, and J. P. Toennies, Surf. Sci. 128, 191 (1983).

<sup>7</sup>A. Ben-Mizrachi and E. Domany (unpublished). We thank both authors for making available to us their results and a draft of their manuscript.

<sup>8</sup>M. Schick, Prog. Surf. Sci. 11, 245 (1981).

<sup>9</sup>M. Bretz, Phys. Rev. Lett. 38, 501 (1977).

<sup>10</sup>M. J. Tejwani, O. Ferreira, and O. E. Vilches, Phys. Rev. Lett. 44, 152 (1980).

<sup>11</sup>K. D. Miner Jr., M. H. W. Chan, and A. D. Migone, Phys. Rev. Lett. 51, 1465 (1983).

<sup>12</sup>D. R. Nelson and B. I. Halperin, Phys. Rev. B 19, 2457 (1979).

<sup>13</sup>A. F. Moodie, C. E. Warble, and L. S. Williams, J. Am. Ceram. Soc. 49, 676 (1966); A. F. Moodie and C. E. Warble, J. Cryst. Growth, 10, 26 (1971).

<sup>14</sup>J. G. Dash, R. Ecke, J. Stoltenberg, O. E. Vilches, and O. J. Whittemore, Jr., J. Phys. Chem. 82, 1450 (1978).

<sup>15</sup>H. Wiechert, C. Tiby, and H. J. Lauter, J. Phys. C 13, L1039 (1980).

<sup>16</sup>R. F. Buzerak, and R. J. Rollefson, J. Low Temp. Phys. 38, 105 (1980).

<sup>17</sup>H. J. Lauter, C. Tiby, H. Wiechert, and C. Knopp (unpublished). This article reports on a preliminary neutron scattering measurement of Ar/MgO.

<sup>18</sup>J.-P. Coulomb, T. S. Sullivan, and O. E. Vilches, J. Phys. (Paris) (to be published).

<sup>19</sup>S. Ross and H. Clark, J. Am. Chem. Soc. 76, 4291 (1954).

<sup>20</sup>B. B. Fisher and W. G. McMillan, J. Chem. Phys. 28, 549 (1958).

<sup>21</sup>T. Takaishi and M. Mori, J. Chem. Soc. Faraday Trans. I, 68, 1921 (1972).

<sup>22</sup>J. L. Jordan, J. P. McTague, L. Passell, and J. B. Hastings, Bull. Am. Phys. Soc. 28, 874 (1983). J. L. Jordan, Ph.D. thesis, University of California, Los Angeles, 1983.

<sup>23</sup>Cryogenic Technology Inc., Waltham, MA 02154. Our unit has a THOR Cryogenics model 3010 II temperature controller.

<sup>24</sup>MKS Instruments Inc., Burlington, MA 01803.

<sup>25</sup>Kr vapor-pressure data: W. T. Ziegler, D. W. Yarbrough, and J. C. Mullins, *Calculation of the Vapor Pressure and Heats of Vaporization and Sublimation of Liquids and Solids Below One Atmosphere Pressure. VI. Krypton*, Natl. Bur. Stand. Report No. 1, Project A-764 (U.S. G.P.O., Washington, D.C., 1964); Ar vapor-pressure data: W. T. Ziegler, J. C. Mullins, and B. S. Kirk, *Calculation of the Vapor Pressure and Heats of Vaporization and Sublimation of Liquids and Solids, Especially Below One Atmosphere Pressure. II. Argon*, Natl. Bur. Stand. Report No. 2, Project A460 (U.S. G.P.O., Washington, D.C., 1971); Xe vapor-pressure data: W. T. Ziegler, J. C. Mullins, and A. R. Berquist, *Calculation of the Vapor Pressure and Heats of Vaporization and Sublimation of Liquids and Solids Below One Atmosphere Pressure. VII. Xenon*, Natl. Bur. Stand. Report No. 3, Project Nos. A-764 and E-115, (U.S. G.P.O., Washington, D.C. 1971).

<sup>26</sup>T. Takaishi and Y. Sensui, Trans. Farad. Soc. 59, 2503 (1963).

<sup>27</sup>F. Millot, Y. Larher, and C. Tessier, J. Chem. Phys. 76, 3327 (1982).

<sup>28</sup>A. Thomy and X. Duval, J. Chim. Phys. 67, 1101 (1970).

<sup>29</sup>J. A. Litzinger and G. A. Stewart, in *Ordering in Two Dimensions*, edited by S. K. Sinha (Elsevier, New York 1980), p. 267.

<sup>30</sup>E. M. Hammonds, P. Heiney, P. W. Stephens, R. J. Bir-

- geneau, and P. Horn, in *Ordering in Two Dimensions*, Ref. 29, p. 29.
- <sup>31</sup>J. P. McTague, J. Als-Nielsen, J. Bohr, and M. Nielsen, *Phys. Rev. B* **25**, 7765 (1982).
- <sup>32</sup>Y. Nardon and Y. Larher, *Surf. Sci.* **42**, 299 (1974).
- <sup>33</sup>G. L. Pollack, *Rev. Mod. Phys.* **36**, 748 (1964).
- <sup>34</sup>A. D. Migone, Z. R. Li, and M. H. W. Chan, *Phys. Rev. Lett.* **53**, 810 (1984); A. D. Migone, Ph.D. thesis, Pennsylvania State University, 1984, unpublished.
- <sup>35</sup>J. Dericbourg, *Surf. Sci.* **59**, 554 (1976).
- <sup>36</sup>M. Nielson and J. P. McTague, *Phys. Rev. B* **19**, 3096 (1979).
- <sup>37</sup>J. Stoltenberg and O. E. Vilches, *Phys. Rev. B* **22**, 2920 (1980).
- <sup>38</sup>J. G. Dash and R. D. Puff, *Phys. Rev. B* **24**, 295 (1981).
- <sup>39</sup>R. E. Ecke, J. G. Dash, and R. D. Puff, *Phys. Rev. B* **26**, 1288 (1982).
- <sup>40</sup>L. W. Bruch, J. Unguris, and M. B. Webb, *Surf. Sci.* **87**, 437 (1979).
- <sup>41</sup>J. G. Dash, *Films on Solid Surfaces* (Academic, New York, 1975), Chap. 5. This chapter contains calculations of the isosteric heat for various models although formula (3) was not specifically derived there (J. G. Dash, private communication).
- <sup>42</sup>J. Regnier, A. Thomy, and X. Duval, *J. Colloid Interface Sci.* **70**, 105 (1979).